SIAM J. Applied Dynamical Systems
Vol. 8, No. 2, pp. 624–640

The Two-Fold Singularity of Discontinuous Vector Fields*

M. R. Jeffrey† and A. Colombo‡

Abstract. When a vector field in $\mathbb{R}^3$ is discontinuous on a smooth codimension one surface, it may be simultaneously tangent to both sides of the surface at generic isolated points (singularities). For a piecewise-smooth dynamical system governed by the vector field, we show that the local dynamics depends on a single quantity—the jump in direction of the vector field through the singularity. This quantity controls a bifurcation, in which the initially repelling singularity becomes the apex of a pair of parabolic invariant surfaces. The surfaces are smooth except where they intersect the discontinuity surface, and they divide local space into regions of attraction to, and repulsion from, the singularity.

Key words. Filippov, sliding, singularity, nonsmooth, discontinuous

AMS subject classifications. 34C23, 37G10, 37G35

DOI. 10.1137/08073113X

1. Introduction.

A piecewise-smooth dynamical system contains discontinuities that approximate sudden changes in the governing vector field. These systems have enjoyed widespread application in recent years, from control theory and nonlinear oscillators to economics and biology. Nevertheless, research into the theory of piecewise-smooth dynamics is at a relatively early stage.

Such systems consist of a finite set of ordinary differential equations,

$$\dot{\mathbf{X}} = \mathbf{G}^i(\mathbf{X}), \qquad \mathbf{X} \in R^i \subset \mathbb{R}^n, \tag{1.1}$$

whose right-hand sides are vector fields $\mathbf{G}^i$ defined on disjoint regions R^i and smoothly extendable to the closure of R^i. The R^i are separated by an $n-1$ dimensional set Σ which we call the *switching surface*. The union of Σ and all R^i covers $\mathbb{R}^n$. The literature in real-world piecewise-smooth problems is now extensive, and we refer the reader to [2, 3, 6, 7, 10] for an overview. Our concern will be vector fields with no constraint on the degree of discontinuity across the switching surface, so-called Filippov systems [5], where the continuous flow defined by (1.1) may be nondifferentiable and irreversible, and may contain *sliding* orbits which are confined to the switching surface.

The theory of singularities in piecewise-smooth systems has proven to be a rich source of novel dynamics, particularly near points where the vector field is tangent to the switching

*Received by the editors July 24, 2008; accepted for publication (in revised form) by J. Meiss February 20, 2009; published electronically May 14, 2009.
http://www.siam.org/journals/siads/8-2/73113.html
†Applied Nonlinear Mathematics Group, Department of Engineering Mathematics, University of Bristol, Queen's Building, University Walk, Bristol BS8 1TR, UK (mike.jeffrey@bristol.ac.uk). The work of this author was supported by the EPSRC grant Making It Real.
‡DEI, Politecnico di Milano, Via Ponzio 34/5, 20133 Milano, Italy (alessandro.colombo@polimi.it). With thanks to the hospitality of the University of Bristol during this work.

surface [3, 4, 11], commonly referred to as "fold" points where the surface is smooth. Here we discuss a particular problem at the very heart of nonsmooth dynamics—points where a vector field is tangent to both sides of a switching surface in systems of three dimensions. This "two-fold" problem has been most notably brought to the fore by Teixeira [14, 15, 16], including a case we call the "Teixeira singularity" which epitomizes the current state of nonsmooth singularity theory. In [15], the Teixeira singularity is shown to violate conditions set out for a particular definition of structural stability in a nonsmooth system, and asymptotic stability is determined only under limited conditions of hyperbolicity. This singularity is our main subject of interest because, despite these results, confusion still surrounds this pivotal point of nonsmooth dynamics.

The reason is that much of our intuition fails in the face of discontinuities. Indeed, there is not yet even a consensus on the definition of topological equivalence in nonsmooth systems, or how definitions of structual stability (e.g., [1, 7, 10, 12, 15]) reflect the robustness of dynamics in a nonsmooth model. Here we study the dynamics directly, without reliance on these definitions, revealing explicit behavior that should be reflected in general theories on structural stability.

Adopting a transparent geometric approach, we study the dynamics around the Teixeira singularity and reveal the simplicity characterizing its local behavior. The interesting case is when the flows of two fields $\mathbf{G}^i$ and $\mathbf{G}^j$ on either side of Σ consist locally of orbits which always return to Σ, spiraling around the singularity between impacts and giving rise to intricate dynamics (see Figure 1). Then the dynamics depends on the relative directions of the vector fields $\mathbf{G}^i$ and $\mathbf{G}^j$ at the singularity, that is, the quantity $\tan\theta^i/\tan\theta^j$, where $\theta^{i,j}$ are the angles subtended by $\mathbf{G}^{i,j}$ at the singularity, to an arbitrary reference direction in Σ. When $\mathbf{G}^i$ and $\mathbf{G}^j$ are antiparallel at the singularity, a bifurcation takes place: on one side of the bifurcation all local trajectories reach the sliding region of Σ in finite time, and on the other side two invariant manifolds separate the local state space into regions of attraction to, and repulsion from, the singularity.

In section 2 we state the problem in terms of standard concepts and state the central result, Theorem 1. In section 3 we provide a local coordinate expression. In section 4 we derive a map that essentially treats the switching surface as a Poincaré section of the flow, revealing a bifurcation of invariant manifolds and proving the theorem. Dynamics on the invariant manifolds is studied in section 5. The preservation of straight lines in the system is key to dealing with the discontinuity, exposing a strict relation between dynamics crossing the switching surface and sliding dynamics on the switching surface which is found in section 6. Near the bifurcation small nonlinear effects must be included, as discussed in section 7.

2. The two-fold problem.

Consider a region in which the vector field (1.1) is discontinuous along a smooth codimension one switching surface Σ. Let

$$\Sigma = \left\{\mathbf{X} \in \mathbb{R}^3 : h(\mathbf{X}) = 0\right\} \tag{2.1}$$

in terms of a scalar valued function $h(\mathbf{X})$.

Definition 1. *In a dynamical system*

$$\dot{\mathbf{X}} = \left\{\dot{\mathbf{X}}^+(\mathbf{X}) \text{ for } h(\mathbf{X}) > 0,\ \dot{\mathbf{X}}^-(\mathbf{X}) \text{ for } h(\mathbf{X}) < 0\right\},$$

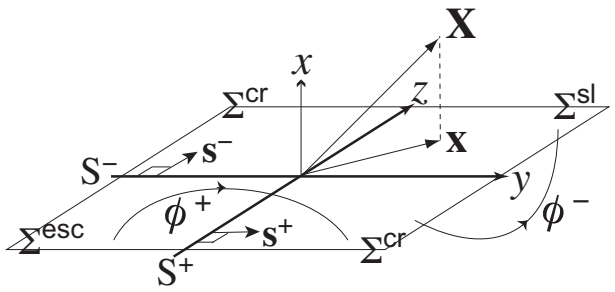

Figure 1. *Coordinates and tangency sets.*

where $\dot{\mathbf{X}}^{\pm} \in \mathbb{R}^3$ *are smooth vector fields, a point* $\mathbf{X}_p \in \Sigma$ *is a two-fold singularity if*

$$\dot{\mathbf{X}}^{\pm}(\mathbf{X}_p) \cdot \nabla h(\mathbf{X}_p) = 0 \quad \textit{and} \quad (\dot{\mathbf{X}}^{\pm}(\mathbf{X}_p) \cdot \nabla)^2 h(\mathbf{X}_p) \neq 0. \tag{2.2}$$

We begin with a local coordinate description of a three dimensional piecewise-smooth dynamical system in which the two-fold singularity is generic. In the neighborhood of any point on Σ, we can choose a coordinate x perpendicular to Σ such that

$$\Sigma = \left\{ \mathbf{X} \in \mathbb{R}^3 : x = 0 \right\}. \tag{2.3}$$

We can distinguish coordinates (y, z) in Σ by writing a general vector in $\mathbb{R}^3$ as

$$\mathbf{X} = [x, \mathbf{x}] = [x, (y, z)], \qquad \mathbf{x} \in \mathbb{R}^2. \tag{2.4}$$

The corresponding dynamical system is

$$\dot{\mathbf{X}} = \left\{ \begin{array}{ll} [\dot{x}^+(\mathbf{X}),\ \dot{\mathbf{x}}^+(\mathbf{X})], & x > 0 \\ [\dot{x}^-(\mathbf{X}),\ \dot{\mathbf{x}}^-(\mathbf{X})], & x < 0 \end{array} \right\}. \tag{2.5}$$

Generically, there exist tranverse $n-2$ dimensional *tangency sets* $S^{\pm}$ given by

$$S^{\pm} = \left\{ \mathbf{X} \in \Sigma : \dot{x}^{\pm} = 0 \right\}. \tag{2.6}$$

We can choose the $\mathbf{x} = (y, z)$ coordinates such that

$$S^+ = \{\mathbf{X} \in \Sigma : y = 0\}, \qquad S^- = \{\mathbf{X} \in \Sigma : z = 0\}; \tag{2.7}$$

see Figure 1. The tangency sets $S^{\pm}$ are perpendicular in these coordinates, intersecting at the *singularity* $p \in \Sigma$ where the x component of both vector fields vanishes, $\dot{x}_p^{\pm} = 0$, at $x = y = z = 0$. They possess unique (up to sign) normal unit vectors $\mathbf{S}^{\pm} = [0, \mathbf{s}^{\pm}]$ satisfying $\mathbf{S}^+ \times \mathbf{S}^- \neq 0$.

The tangency sets partition Σ into four regions. Where $\dot{x}^+ < 0 < \dot{x}^-$ we have the *sliding* region Σ^{sl}, and where $\dot{x}^- < 0 < \dot{x}^+$ we have the *escaping* (or "unstable sliding") region Σ^{esc}. If we choose the sign of $\mathbf{s}^{\pm}$ such that $\dot{\mathbf{x}}^{\pm} \cdot \mathbf{s}^{\pm} > 0$ (as in Figure 1), these can be written as

$$\Sigma^{\mathsf{sl}} = \left\{ \mathbf{x} \in \Sigma : \mathbf{s}^{\pm} \cdot \mathbf{x} \geq 0 \right\}, \qquad \Sigma^{\mathsf{esc}} = \left\{ \mathbf{x} \in \Sigma : \mathbf{s}^{\pm} \cdot \mathbf{x} < 0 \right\}. \tag{2.8}$$

Orbits pass from one flow to the other by traversing Σ in the two *crossing* (or "sewing") regions

$$\Sigma^{\mathsf{cr}} = \left\{ \mathbf{x} \in \Sigma : \mathbf{s}^+ \cdot \mathbf{x} < 0 \leq \mathbf{s}^- \cdot \mathbf{x} \ \text{ or } \ \mathbf{s}^- \cdot \mathbf{x} < 0 \leq \mathbf{s}^+ \cdot \mathbf{x} \right\}. \tag{2.9}$$

Throughout this paper we distinguish between "orbits" that may meet the switching surface only in Σ^{cr} and "sliding orbits" that are contained in $\Sigma^{\mathsf{sl,esc}}$. More precisely, we give the following definition based on [1].

Definition 2.

- *An* orbit *is a piecewise-smooth curve $\gamma \subset \mathbb{R}^3$ whose segments in $x > 0$ are trajectories of $\dot{\mathbf{X}} = \dot{\mathbf{X}}^+$ and whose segments in $x < 0$ are trajectories of $\dot{\mathbf{X}} = \dot{\mathbf{X}}^-$, whose intersections with $x = 0$ consist of crossing points or tangency points, such that γ is maximal with respect to these two conditions.*
- *A* sliding orbit *is a smooth curve $\gamma \subset \Sigma$ such that γ is a trajectory of the Filippov sliding vector field expressed in* (6.1)–(6.2).

Two-folds may contain two different forms of tangency point.

Definition 3. *Tangency of the vector field to Σ is*

- visible *on $S^{\pm}$ if* $\mathsf{sign}\,(\ddot{x}^{\pm}) = \pm 1$, *and*
- invisible *on $S^{\pm}$ if* $\mathsf{sign}\,(\ddot{x}^{\pm}) = \mp 1$.

That is, "visible" implies that the orbit tangent to Σ at S^+ (or S^-) extends locally into the region $x > 0$ (or $x < 0$). We will refer to a two-fold singularity consisting of two coincident invisible tangencies as the *Teixeira singularity*. In this case both the smooth flows of $\dot{\mathbf{X}}^{\pm}$ consist locally of orbits which always return to Σ, spiraling around the singularity between impacts, giving rise to intricate dynamics. Then we may define a second-return map ϕ that maps a point from Σ, through one smooth vector field until it hits Σ, and then through the other vector field until it impacts Σ again. The following have been proven in [15].

T1: The two-fold singularity is *structurally stable* if and only if at least one of the tangency sets is visible. Thus the Teixeira singularity is structurally unstable.

T2: The Teixeira singularity is *asymptotically stable* provided that (i) the second-return map ϕ is hyperbolic, and (ii) the Filippov sliding vector field is hyperbolic with the phase portrait of an attracting node and the eigendirection associated with the eigenvalue of smaller absolute value in the sliding region Σ^{sl}.

Structural stability of a piecewise-smooth system, defined in [1, 3, 9], in short requires that orbits, sliding orbits, and switching surfaces of a system be mapped through a homeomorphism onto those of all neighboring systems in the parameter space. T2 is a paraphrasing of the statement "the U[Teixeira]-singularity is asymptotically stable provided that it is an S-singularity," and for a precise definition we refer the reader to [15]. We will define the Filippov sliding vector field in (6.1).

In the cases where at least one of the tangency sets is visible, the dynamics is rather straightforward, and asymptotic stability then relies only on the form of the Filippov sliding vector field, which has been further considered in [16]. Henceforth we will be interested only in the case of coincident invisible tangencies, the Teixeira singularity. According to T1 and T2, the Teixeira singularity is structurally unstable, with asymptotic stability determinable only when the return map and Filippov field are hyperbolic.

Our aim is to shed light on this problem without recourse to T1 and T2 by an explicit study of the local dynamics. We will show that the vector field is indeed structurally unstable at a certain parameter value and unfold the resulting bifurcation. This allows us to determine regions over which the singularity is attracting or repelling. This last issue must be considered with care, since the singularity is not a stationary point of the vector field. The convergence of sliding orbits upon the singularity causes confusion over the local dynamics, which we will study in detail, revealing regions of attraction to and repulsion from the singularity instead of asymptotic stability.

The central result, which will be proven in section 4, is the following theorem.

Theorem 1. *A two-fold singularity can be expressed in a local approximation as*

$$\dot{\mathbf{X}} = \left\{ \dot{\mathbf{X}}^+ \text{ for } x > 0,\ \dot{\mathbf{X}}^- \text{ for } x < 0 \right\}$$

in coordinates $\mathbf{X} = [x, y, z]$, *where* $\Sigma = \left\{ \mathbf{X} \in \mathbb{R}^3 : x = 0 \right\}$, *and*

$$\dot{\mathbf{X}}^+ = \left[-ya, 1, V^+ \right], \qquad \dot{\mathbf{X}}^- = \left[zb, V^-, 1 \right] \tag{2.10}$$

for $a, b, V^\pm \in \mathbb{R}$. *For the Teixeira singularity* $a, b > 0$, *this satisfies the following:*

(i) *If* $V^+V^- > 1$ *and* $V^\pm < 0$, *every orbit of* (2.10) *crosses* Σ *an infinite number of times. There exist a pair of invariant surfaces that meet at the singularity.*

(ii) *If* $V^+V^- < 1$ *or* $V^+ > 0$ *or* $V^- > 0$, *every orbit of* (2.10) *crosses* Σ *a finite number of times.*

A bifurcation takes place at $V^+V^- = 1$ for $V^\pm < 0$. Furthermore, the following will be shown.

(i) If $V^+V^- > 1$ and $V^\pm < 0$, one of the invariant surfaces is asymptotically attractive, and encloses the escaping region Σ^{esc} within the domain of repulsion of the singularity; the other invariant surface is asymptotically repulsive and encloses the sliding region Σ^{sl} within the domain of attraction of the singularity.

(ii) If $V^+V^- < 1$ or $V^+ > 0$ or $V^- > 0$, sliding orbits are repelled from the singularity, and

(ii.i) if $V^+ > 0$, every orbit crosses Σ at most once from $x < 0$ to $x > 0$,

(ii.ii) if $V^- > 0$, every orbit crosses Σ at most once from $x > 0$ to $x < 0$, and

(ii.iii) if $0 < V^+V^- < 1$ and $V^\pm < 0$, every orbit crosses Σ at least once before impacting the sliding region.

The topology and dynamics of the locally invariant surfaces for (i) will be determined in sections 4–5.

3. Local approximation.

To determine the fate of orbits in the neighborhood of the singularity, we derive a local approximation for the vector field. First, local cubic tangencies to Σ are prohibited by conditions

$$\ddot{x}^+ < 0, \qquad \ddot{x}^- > 0, \tag{3.1}$$

and there are assumed to be no local equilibria, i.e., $\dot{\mathbf{X}}^\pm \neq 0$. Under these assumptions, in a sufficiently small neighborhood of the singularity, the vector fields' projection onto the

switching surface Σ is approximately constant. That is, by a Taylor expansion up to linear order in the x-direction and zeroth order in the y, z-directions, we can express the vector field as

$$\left[\dot{x}^+, \dot{\mathbf{x}}^+\right] \approx \left[-ya, \mathbf{v}^+\right], \qquad \left[\dot{x}^-, \dot{\mathbf{x}}^-\right] \approx \left[zb, \mathbf{v}^-\right], \tag{3.2}$$

where $\mathbf{v}^+ = (1, V^+)$ and $\mathbf{v}^- = (V^-, 1)$ are nonzero vector constants, and $a, b > 0$. Henceforth we can set $a = b = 1$ without loss of generality. More details are given in the appendix.

The flows of each vector field in this parabolic approximation map points on Σ, through the smooth regions $x > 0$ and $x < 0$, to return points on Σ according to

$$\phi^+ : \{\Sigma : y < 0\} \mapsto \{\Sigma : y > 0\}, \qquad \phi^- : \{\Sigma : z < 0\} \mapsto \{\Sigma : z > 0\} \tag{3.3}$$

and given explicitly by

$$\phi^+ : \mathbf{x} \mapsto \mathbf{x} - 2y\mathbf{v}^+, \qquad \phi^- : \mathbf{x} \mapsto \mathbf{x} - 2z\mathbf{v}^-. \tag{3.4}$$

As observed by Teixeira [15], this deceptively simple map is the key to understanding coincident invisible tangencies. In what follows we study its geometry.

The overlap of the domains of $\phi^\pm$ is the *escaping* region Σ^{esc}, and the overlap of their ranges is the *sliding* region Σ^{sl}.

The local dynamics is given by an alternating series of iterations of the maps ϕ^+ and ϕ^-. Any point on the escaping region can only be a start point of the series, and any point in the sliding region can only be an end point of the series. The term "escaping" refers to the fact that, arbitrarily close to Σ^{esc} with $x \neq 0$, orbits of $\dot{\mathbf{X}}^\pm$ move away from Σ^{esc}. In this section we will regard points *arbitrarily close* to Σ^{esc} as in fact being *on* Σ^{esc}. In section 6, we will deal with the sliding orbits that apply to points exactly *in* Σ^{esc} with $x = 0$. Our goal here is to understand under what conditions all points on the escaping and crossing regions eventually reach the sliding region, and what happens when these conditions are not met.

To label points on Σ let $m \in \mathbb{Z}$, then let every $\mathbf{x}_{2m}$ be mapped by ϕ^+, and let every $\mathbf{x}_{2m-1}$ be mapped by ϕ^-, so that

$$\mathbf{s}^+ \cdot \mathbf{x}_{2m} < 0, \qquad \mathbf{s}^- \cdot \mathbf{x}_{2m-1} < 0. \tag{3.5}$$

We can rewrite the maps (3.4) locally as oblique reflections in the line $S^\pm$:

$$\phi^+ : \begin{cases} \dfrac{\mathbf{x}_{2m+1} - \mathbf{x}_{2m}}{|\mathbf{x}_{2m+1} - \mathbf{x}_{2m}|} = \dfrac{\mathbf{v}^+}{|\mathbf{v}^+|}, \\ \mathbf{s}^+ \cdot (\mathbf{x}_{2m+1} + \mathbf{x}_{2m}) = 0, \end{cases} \qquad \phi^- : \begin{cases} \dfrac{\mathbf{x}_{2m} - \mathbf{x}_{2m-1}}{|\mathbf{x}_{2m} - \mathbf{x}_{2m-1}|} = \dfrac{\mathbf{v}^-}{|\mathbf{v}^-|}, \\ \mathbf{s}^- \cdot (\mathbf{x}_{2m} + \mathbf{x}_{2m-1}) = 0. \end{cases} \tag{3.6}$$

The upper condition specifies that the direction of reflection is $\mathbf{v}^\pm$, while the lower condition specifies that the start and end points have the same perpendicular distance from $S^\pm$. This is illustrated in Figure 2. Projecting the upper equation along $\mathbf{s}^+$ (for ϕ^+) or $\mathbf{s}^-$ (for ϕ^-) and then eliminating the quantities $|\mathbf{x}_{i+1} - \mathbf{x}_i|$, we obtain

$$\mathbf{x}_{2m+1} - \mathbf{x}_{2m} = -2\frac{\mathbf{s}^+ \cdot \mathbf{x}_{2m}}{\mathbf{s}^+ \cdot \mathbf{v}^+}\mathbf{v}^+, \qquad \mathbf{x}_{2m} - \mathbf{x}_{2m-1} = -2\frac{\mathbf{s}^- \cdot \mathbf{x}_{2m-1}}{\mathbf{s}^- \cdot \mathbf{v}^-}\mathbf{v}^-. \tag{3.7}$$

Notice that both denominators are equal to 1 as given by (3.2).

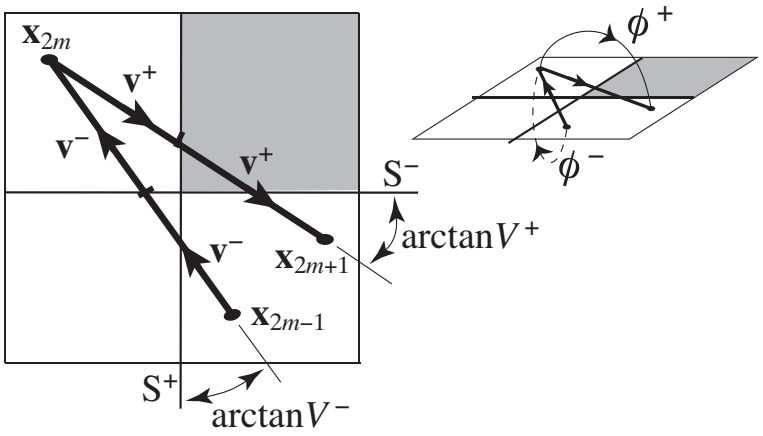

Figure 2. *Local mapping: In the parabolic approximation, points are reflected in S^+ and S^-. In this example the point $\mathbf{x}_{2m-1}$ is reflected obliquely in S^- to $\mathbf{x}_{2m}$, and then in S^+ to $\mathbf{x}_{2m+1}$, remaining in the crossing regions. The sliding region is shaded.*

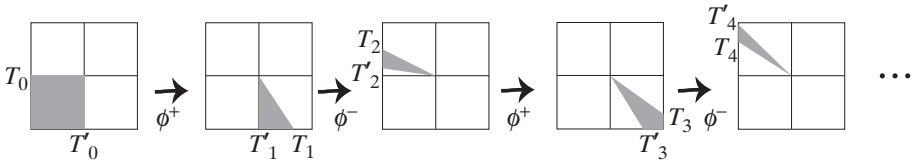

Figure 3. *The first four iterates of the escaping region on Σ. In this example they map repeatedly into the crossing regions.*

It is tempting to consider these two dimensional maps in their obvious cartesian form, but it is not clear how to apply principles of asymptotic stability from smooth dynamical systems. For example, Teixeira [15] remarks that the second-return map $\mathbf{x}_m \mapsto \mathbf{x}_{m+2}$ (the map $\phi^+ \circ \phi^-$ or $\phi^- \circ \phi^+$) is nonhyperbolic if, in the notation of Theorem 1, $0 < V^+V^- < 1$. It is unclear whether this condition says anything about the stability of the system because orbits only cross Σ over a finite time period before entering the sliding region.

Instead we can exploit the fact that the maps (3.7) preserve straight lines through the origin. That is, any point on the line $\mathbf{x}_{2m} = R(\cos\theta_{2m}, \sin\theta_{2m})$ for $R \in \mathbb{R}$ variable maps to a point on another line, $\mathbf{x}_{2m+1} = R'(\cos[\theta_{2m} + f(\theta_{2m})], \sin[\theta_{2m} + f(\theta_{2m})])$. So to study the images of Σ^{sl} and Σ^{esc} under successive iterations of $\phi^{\pm}$, we need only consider the rotation of their boundaries, which are straight lines through the origin, as illustrated in Figure 3. This rotation constitutes the angular behavior of (3.7). In the next section we shall see that, under certain conditions, this angular map has two fixed points, corresponding to invariant manifolds of the second return map derived from (3.7). In section 5 we will study the radial behavior of (3.7) restricted to the two invariant manifolds.

4. The tangent map.

Let us introduce the quantities

$$T_{2m} = \frac{\mathbf{s}^- \cdot \mathbf{x}_{2m}}{\mathbf{s}^+ \cdot \mathbf{x}_{2m}}, \qquad T_{2m-1} = \frac{\mathbf{s}^+ \cdot \mathbf{x}_{2m-1}}{\mathbf{s}^- \cdot \mathbf{x}_{2m-1}}, \tag{4.1}$$

which are, respectively, the tangent T_{2m} of the angle made with $\mathbf{s}^+$ by a vector $\mathbf{x}_{2m}$ in the domain of ϕ^+ and the tangent T_{2m-1} of the angle made with $\mathbf{s}^-$ by a vector $\mathbf{x}_{2m-1}$ in the domain of ϕ^-. These domains are defined in (3.3). We define corresponding quantities for the vectors $\mathbf{v}^\pm$ as

$$V^+ = \frac{\mathbf{s}^- \cdot \mathbf{v}^+}{\mathbf{s}^+ \cdot \mathbf{v}^+}, \qquad V^- = \frac{\mathbf{s}^+ \cdot \mathbf{v}^-}{\mathbf{s}^- \cdot \mathbf{v}^-}. \tag{4.2}$$

T_m is positive for points $\mathbf{x}_m$ in the escaping and sliding regions, negative in the crossing regions, and zero on the boundary of Σ^{esc}. Moreover, it is well defined, except on the boundary of Σ^{sl} (where sliding dynamics apply; see section 6), whereas $V^\pm$ are always well defined due to conditions (3.1).

From (3.7) and (4.1)–(4.2) we obtain maps for T_{2m} and T_{2m-1}:

$$T_{2m+1} = \frac{1}{2V^+ - T_{2m}}, \qquad T_{2m} = \frac{1}{2V^- - T_{2m-1}}. \tag{4.3}$$

Clearly, a positive V^+ or V^- implies that points in the crossing regions ($T_m < 0$) are mapped into the sliding region ($T_m > 0$) after at most two iterations, or one iteration if both $V^\pm$ are positive. More precisely, note that an iterate of (4.3) lies in the crossing regions only if it satisfies

$$2V^+ < T_{2m} < 0, \qquad 2V^- < T_{2m-1} < 0. \tag{4.4}$$

We therefore have the following lemma.

Lemma 4.1. *The following statements hold for the Teixeira singularity, as expressed in* (2.10) *with* $a, b > 0$*:*

(i) *if* $V^+ > 0$*, every orbit crosses* Σ *at most once from* $x < 0$ *to* $x > 0$*,*
(ii) *if* $V^- > 0$*, every orbit crosses* Σ *at most once from* $x > 0$ *to* $x < 0$*, and*
(iii) *if* $0 < V^+V^- < 1$ *and* $V^\pm < 0$*, every orbit crosses* Σ *at least once before impacting the sliding region.*

Proof.

(i) If $V^+ > 0$, (4.4) implies that any T_{2m} is mapped by (4.3) to $T_{2m+1} > 0$, a termination point in the sliding region. Therefore, there is at most one crossing point T_{2m} in the region $y < 0 < z$, where orbits cross from $x < 0$ to $x > 0$.

(ii) If $V^- > 0$, (4.4) implies that any T_{2m-1} is mapped by (4.3) to $T_{2m} > 0$, a termination point in the sliding region. Therefore, there is at most one crossing point T_{2m-1} in the region $z < 0 < y$, where orbits cross from $x > 0$ to $x < 0$.

(iii) If $0 < V^+V^- < 1$ and $V^\pm < 0$, then for any $T_m > 0$ we have from (4.3) that

$$T_{m+1} = \frac{1}{2V^\pm - T_m} = \frac{1}{-2\,|V^\pm| - |T_m|} < 0 \tag{4.5}$$

for V^+ if m is even or V^- if m is odd. Therefore, an iterate T_m exists for all orbits; thus there always exists at least one crossing point. ∎

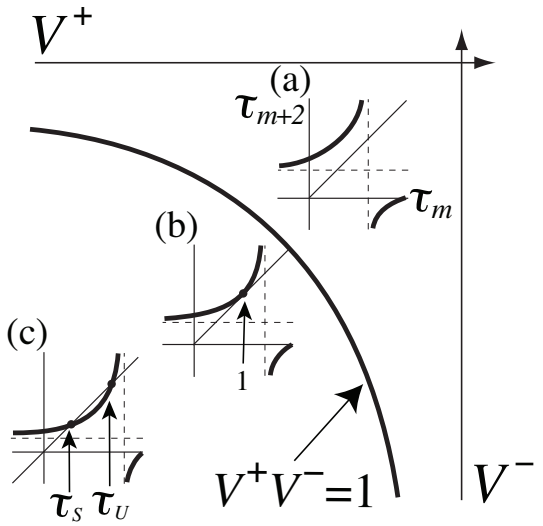

Figure 4. *Tangent mapping and bifurcation diagram:* (a) *No invariant manifolds for* $V^+V^- < 1$, (b) *bifurcation along* $V^+V^- = 1$, (c) *two fixed points* $\tau_S = \tau_\star$ *and* $\tau_U = 1/(\tau_\star V^+V^-)$ *in* $V^+V^- > 1$. $\tau_m = 0$ *is the boundary of* Σ^{esc}. *Lines with* $\tau_m = 2 - 1/(2V^+V^-)$ *map to the* τ_{m+2} *graph asymptotes (dashed) which are the boundaries of* Σ^{sl}. *The bound* $\tau_m < 2$ *ensures the existence of the intermediate step* τ_{m+1}.

More insight is given by the second-return maps ($T_{2m} \mapsto T_{2m+1}$ followed by $T_{2m+1} \mapsto T_{2m+2}$ and vice versa). These are a pair of Möbius transformations expressible concisely as

$$\tau_{m+2} = \frac{\tau_m - 2}{2V^+V^-(\tau_m - 2) + 1} \tag{4.6}$$

for $T_{2m} = V^+\tau_{2m}$ and $T_{2m-1} = V^-\tau_{2m-1}$, shown in Figure 4. For this to make sense, the intermediate $(m+1)$th iterate must lie in the crossing region, limiting the angle subtended by T_m to the boundaries of the escaping region, with the conditions (4.4).

From this second-return map (4.6) we have the result as stated in Theorem 1:

(i) *If* $V^+V^- > 1$ *and* $V^\pm < 0$, *every orbit of* (2.10) *crosses* Σ *an infinite number of times. There exist a pair of invariant surfaces that meet at the singularity.*

(ii) *If* $V^+V^- < 1$ *or* $V^+ > 0$ *or* $V^- > 0$, *every orbit of* (2.10) *crosses* Σ *a finite number of times.*

Proof of Theorem 1. The local approximation (2.10) is obtained by a constant scaling of the Teixeira singularity vector field given in [15]. Then consider the second-return map (4.6). If $V^+V^- > 1$, the map has two fixed points—one at $\tau_\star$ with eigenvalue $(1 - 2/\tau_\star)^{-2} < 1$ which is therefore stable (asymptotically attracting), and one at $1/(\tau_\star V^+V^-)$ with eigenvalue $(1 - 2V^+V^-\tau_\star)^{-2} > 1$ which is therefore unstable (asymptotically repelling), where

$$\tau_\star = 1 - \sqrt{1 - \frac{1}{V^+V^-}}. \tag{4.7}$$

Note that $\tau_\star > 0$ and $1/(\tau_\star V^+V^-) > 0$. Then the following hold:

(i) If $V^+V^- > 1$ and $V^\pm < 0$, the equilibria $V^\pm\tau_\star < 0$ and $V^\pm/(\tau_\star V^+V^-) < 0$, of the $T_m \mapsto T_{m+2}$ maps from (4.6), lie in the crossing regions. From (4.6), the $T_m \mapsto T_{m+2}$ maps are monotonic; therefore, all trajectories tend asymptotically toward the equilibria either in forward or in reverse time and thus cross Σ an infinite number of times. The smooth segments of orbits starting and ending at crossing points along the $\{T_m, T_{m+1}\}$ directions thus form invariant surfaces; the surfaces intersect Σ along lines through the singularity given by $\mathbf{x} = l\,(1, V^+\tau_\star)$ and $\mathbf{x} = l\,(1, V^+/(\tau_\star V^+V^-))$ for $l \in \mathbb{R}$.

(ii) If $V^+V^- > 1$ and $V^\pm > 0$, then the equilibria $V^+\tau_\star > 0$ and $V^\pm/(\tau_\star V^+V^-) > 0$, of the $T_m \mapsto T_{m+2}$ maps, lie in the sliding or escaping regions, so the equilibria are outside of the range of (4.6). If $V^+V^- < 1$, there are no real-valued equilibria. In either case there are then no admissible limit points (i.e., in the crossing regions), so all trajectories intersect the sliding and escaping regions after finitely many iterations. ■

More explicitly, from (4.7), the maps $T_{2m} \mapsto T_{2m+2}$ and $T_{2m-1} \mapsto T_{2m+1}$, respectively, have stable equilibria T_S^+ and T_S^- given by

$$\frac{T_S^+}{V^+} = \frac{T_S^-}{V^-} = 1 - \sqrt{1 - \frac{1}{V^+V^-}} \tag{4.8}$$

and unstable equilibria T_U^+ and T_U^- given by

$$\frac{T_U^+}{V^+} = \frac{T_U^-}{V^-} = 1 + \sqrt{1 - \frac{1}{V^+V^-}}. \tag{4.9}$$

These exist only in the crossing regions, $T_{U,S}^\pm < 0$; otherwise, we have one of the cases where V^+ or V^- are positive. They are invariant manifolds of the second-return maps derived from (3.7). From (4.4) it is clear that they divide Σ such that the stable manifolds $T_S^\pm$ enclose the escaping region, while the unstable manifolds $T_U^\pm$ enclose the sliding region. It is easy to show from (4.8)–(4.9) that each pair $\{T_S^+, T_U^-\}$ and $\{T_U^+, T_S^-\}$ forms a straight line through the origin since $T_S^\pm T_U^\mp = 1$.

At $V^+V^- = 1$, the invariant manifolds of each map coalesce and annihilate in what we refer to as the "nonsmooth diabolo" bifurcation for reasons that will become apparent.

5. Dynamics on the invariant manifolds. Now consider the dynamics of points on the invariant manifolds (4.8)–(4.9). A point $\mathbf{x}_m$ has radial coordinate

$$R_m = \sqrt{(\mathbf{s}^+ \cdot \mathbf{x}_m)^2 + (\mathbf{s}^- \cdot \mathbf{x}_m)^2}. \tag{5.1}$$

By combining this with (3.7) and iterating twice (and using (4.6) to simplify), we find the radial maps

$$\begin{aligned} R_{2m+2}^2 &= \frac{1 + T_{2m+2}^2}{1 + T_{2m}^2}\left(\frac{2V^+ - T_{2m}}{T_{2m+2}}\right) R_{2m}^2, \\ R_{2m+1}^2 &= \frac{1 + T_{2m+1}^2}{1 + T_{2m-1}^2}\left(\frac{2V^- - T_{2m-1}}{T_{2m+1}}\right) R_{2m-1}^2, \end{aligned} \tag{5.2}$$

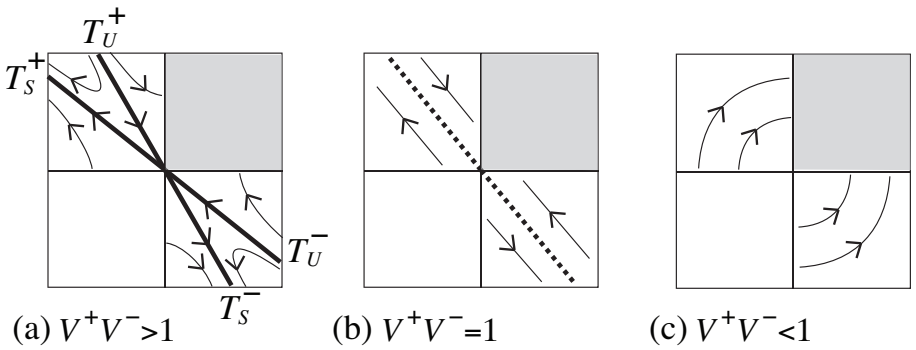

Figure 5. *Invariant manifold bifurcation:* (a)–(c) *correspond to the parameter values in Figure 4.* (a) $T_S^\pm$ *and* $T_U^\pm$ *form two stable and two unstable manifolds in the crossing regions, which are respectively repelling and attracting with respect to the singularity at the center.* (b) *The manifolds coalesce in a line of fixed points.* (c) *All points map from the escaping region to the sliding region in finite time.*

which on the invariant manifolds simplify to

$$\frac{R_{m+2}}{R_m} = \frac{1 \pm \sqrt{1 - 1/V^+V^-}}{1 \mp \sqrt{1 - 1/V^+V^-}}, \tag{5.3}$$

taking the upper signs for $T_S^\pm$ and the lower signs for $T_U^\pm$. Since $V^+V^- > 1$,

$$\begin{aligned} &R_{m+2} > R_m \quad \text{on the stable manifolds } T_S^\pm, \text{ and} \\ &R_{m+2} < R_m \quad \text{on the unstable manifolds } T_U^\pm. \end{aligned} \tag{5.4}$$

Therefore, points in T_U move toward the singularity, while points in T_S move away from it. This is illustrated in Figure 5.

We can easily extend this picture out of the switching surface Σ, since each $\{\mathbf{x}_m, \mathbf{x}_{m+1}\}$ pair contains the start and end points of a smooth orbit segment in the flow of (3.2). Thus the invariant manifolds form two continuous, parabolic (i.e., quadratic, of the form $x \propto V^+y^2 + V^-z^2 - 2V^+V^-yz$), invariant surfaces U and S, which are smooth except at their intersections $T_U^\pm$ and $T_S^\pm$ with Σ. They form a nonsmooth diabolo (Figure 6), an attractive cone S which encloses Σ^{esc}, and a repelling cone U which encloses Σ^{sl}, both with apex at the origin and nondifferentiable where they intersect Σ at edges along $T_{U,S}^\pm$.

6. Dynamics in the sliding region. We have determined the qualitative dynamics of orbits in the system (3.2), exclusive of any dynamics on the switching surface that occurs before ejection from the escaping region Σ^{esc}, and after impact with the sliding region Σ^{sl}. The system (3.2) does not specify the vector field in these regions.

To address this we adopt the Filippov convention,

$$\dot{\mathbf{X}} = [0, \mathbf{f}] \quad \text{for all } \mathbf{X} \in \Sigma^{\mathsf{sl}} \cup \Sigma^{\mathsf{esc}}, \tag{6.1}$$

where, recalling that we have set $a = b = 1$,

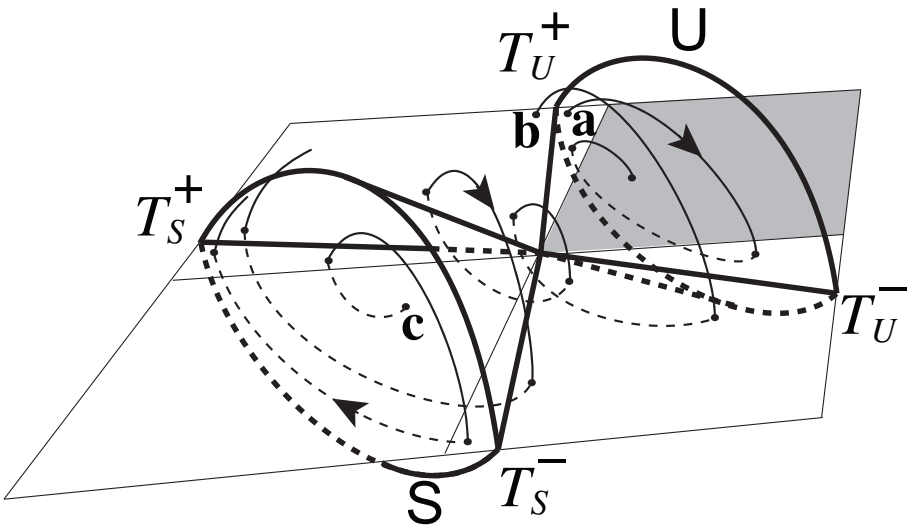

Figure 6. *The nonsmooth diabolo: Invariant manifolds near a two-fold singularity. The three qualitatively different types of orbit are shown.* **a:** *An orbit starting near the inside of* U *spirals in toward the singularity and hits the sliding region (shaded).* **b:** *An orbit starting near the outside of* U *initially spirals inward toward the singularity, then spirals out away from the singularity, and tends asymptotically toward* S. **c:** *An orbit spirals outward from the escaping region and away from the singularity, approaching* S *asymptotically.*

$$\begin{aligned}\mathbf{f} &= \frac{\left(\nabla h \cdot \dot{\mathbf{X}}^-\right)\dot{\mathbf{x}}^+ - \left(\nabla h \cdot \dot{\mathbf{X}}^+\right)\dot{\mathbf{x}}^-}{\nabla h \cdot \left(\dot{\mathbf{X}}^- - \dot{\mathbf{X}}^+\right)} \\ &= \frac{z\mathbf{v}^+ + y\mathbf{v}^-}{z+y}. \end{aligned} \tag{6.2}$$

In the sliding region Σ^{sl} the denominator of (6.2) is strictly positive, so a coordinate transformation that preserves sliding orbits scales out the denominator and we consider locally

$$\tilde{\mathbf{f}} = z\mathbf{v}^+ + y\mathbf{v}^-. \tag{6.3}$$

This has Jacobian determinant

$$\left|\mathsf{D}\,\tilde{\mathbf{f}}\right| = \begin{vmatrix} V^- & 1 \\ 1 & V^+ \end{vmatrix} = V^-V^+ - 1; \tag{6.4}$$

recall that $\mathbf{v}^+ = (1, V^+)$ and $\mathbf{v}^- = (V^-, 1)$. Then,

$$\mathsf{sign}\left|\mathsf{D}\tilde{\mathbf{f}}\right| = \mathsf{sign}\left(V^+V^- - 1\right) = \begin{cases} +1 & \Leftrightarrow \quad T^{\pm}_{U,S} < 0, \\ -1 & \Leftrightarrow \quad T^{\pm}_{U,S} \notin \mathbb{R}. \end{cases} \tag{6.5}$$

The equivalence on the right holds for $V^{\pm} < 0$, the parameter regime where the invariant manifold bifurcation occurs.

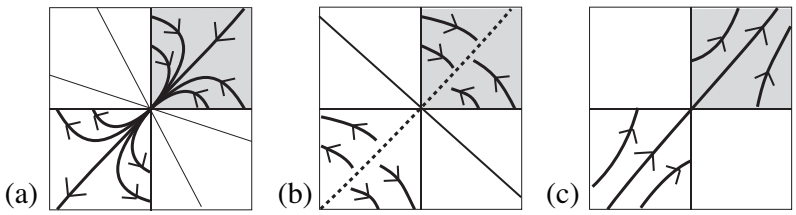

Figure 7. *Sliding dynamics and invariant manifolds.* (a)–(c) *correspond to Figure 5. The normalized sliding vector field (6.3) has* (a) *an attracting node at the singularity for* $V^+V^- > 1$, (b) *a line of equilibria extending from the singularity for* $V^+V^- = 1$, *and* (c) *a saddle at the singularity with unstable manifold in* Σ^{sl} *(shaded) for* $V^+V^- < 1$. *These lead to the true sliding vector field (6.2) as depicted.*

Thus the existence of the invariant manifolds $T^{\pm}_{U,S}$ for $V^+V^- > 1$ coincides with the existence of a node in $\tilde{\mathbf{f}}$ at the singularity. To see that the node is attractive, observe that $\tilde{\mathbf{f}}$ points into the sliding region and $V^{\pm} = \frac{\mathbf{s}^{\pm}\cdot\mathbf{v}^{\pm}}{\mathbf{s}^{\mp}\cdot\mathbf{v}^{\pm}} < 0$, and therefore $V^{\pm} < 0$, so the sum of the eigenvalues of $\mathsf{D}\tilde{\mathbf{f}}$ is simply

$$\mathsf{Tr}\left(\mathsf{D}\tilde{\mathbf{f}}\right) = V^+ + V^- < 0. \tag{6.6}$$

Also from (6.5), the absence of invariant manifolds for $V^+V^- < 1$ coincides with the existence of a saddle in $\tilde{\mathbf{f}}$ at the singularity. The eigenvectors of $\mathsf{D}\tilde{\mathbf{f}}$ are

$$\mathbf{w}_{\pm} = \left(1, \omega_{\pm} - V^-\right), \tag{6.7}$$

and the corresponding eigenvalues are

$$\omega_{\pm} = \tfrac{1}{2}\left(V^+ + V^- \pm \sqrt{(V^+ - V^-)^2 + 4}\right). \tag{6.8}$$

The first component of $\mathbf{w}_{\pm}$ is positive, while the second component is positive for ω_+ and negative for ω_-. That is,

$$\mathbf{w}_+ \in \Sigma^{\mathsf{sl}}, \qquad \mathbf{w}_- \in \Sigma^{\mathsf{cr}}. \tag{6.9}$$

Thus the saddle's unstable separatrix direction $\mathbf{w}_-$ lies in the sliding region, and the stable separatrix direction $\mathbf{w}_+$ lies in the crossing region.

In the exact sliding vector field $\mathbf{f}$ the sliding orbits are the same as the node ($V^+V^- > 1$) and saddle ($V^+V^- < 1$) orbits of $\tilde{\mathbf{f}}$, but they reach/depart the singularity in finite time. That is, the singularity is not an equilibrium point of the sliding vector field $\mathbf{f}$. Furthermore, to obtain the sliding vector field in the escaping region Σ^{esc}, the time direction must be reversed from that of the normalized field. This is illustrated in Figure 7, including the presence of a line of equilibria when $V^+V^- = 1$.

7. Small perturbations near the bifurcation. Here we investigate the effect of nonlinear terms on the local dynamics when $V^+V^- \approx 1$. To understand what happens to the line of equilibria in the sliding region we may appeal to center manifold theory: choose a coordinate

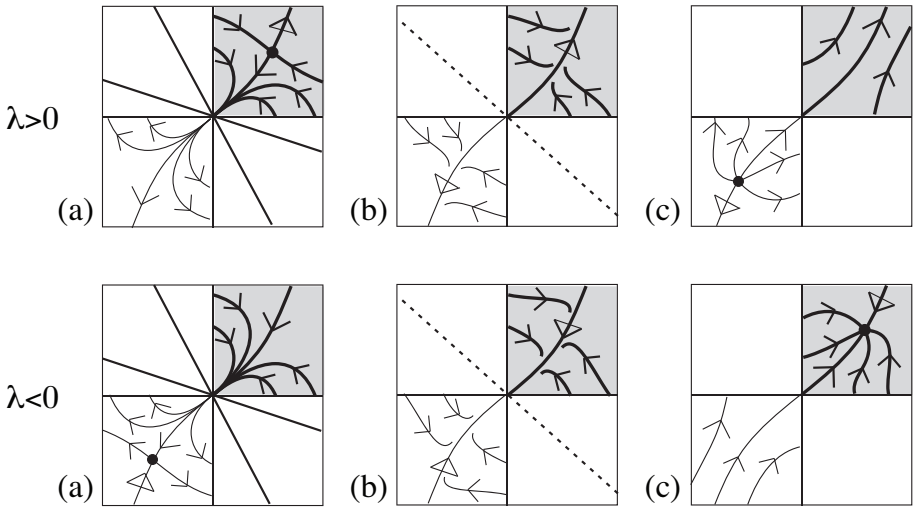

Figure 8. *Perturbed sliding dynamics, showing the effect of positive perturbation $\lambda > 0$ (top) and negative perturbation $\lambda < 0$ (bottom). Triangular arrowheads indicate nonlinear (in)stability.* (a)–(c) *correspond to parameter values in Figure 7.*

u along the center manifold—the line of equilibria in Figure 7(b). The one-dimensional sliding field on the center manifold, $\tilde{f} = \omega_+ u$, is structurally unstable at the bifurcation point $\omega_+ = 0$. A nonlinear perturbation gives the transcritical bifurcation normal form

$$\tilde{f} = \omega_+ u + \lambda u^2. \tag{7.1}$$

This introduces an equilibrium in the sliding region: a saddlepoint that exists when $V^+V^- < 1$ for a positive perturbation $\lambda > 0$, and an attracting node that exists when $V^+V^- > 1$ for a negative perturbation $\lambda < 0$, illustrated in Figure 8. In the escaping region Σ^{esc} the same analysis follows; note that the transformation to $\tilde{\mathbf{f}}$ reverses the time direction there. As we pass through the bifurcation at $V^+V^- = 1$, the field $\tilde{\mathbf{f}}$ undergoes a transcritical bifurcation, as the second equilibrium moves between the sliding and escaping regions. Note, however, that in the true sliding vector field $\mathbf{f}$, the singularity is no longer an equilibrium, and sliding orbits reach it in finite time.

Regarding crossing orbits, the line of fixed points in Figure 5(b) illustrates the presence of a structural instability in the second-return maps, coexisting with the center manifold in the sliding region. This occurs because the condition $V^+V^- = 1$ means that the reflection vectors $(1, V^+)$ and $(V^-, 1)$ are colinear, with the same direction but opposite orientation. A full investigation of higher order behavior is beyond the scope of this paper. One way forward is to consider the effect of higher order terms on the second-return maps. At $V^+V^- = 1$ the eigenvalues of the Jacobians of these maps satisfy the Takens–Bogdanov condition [8, 13] that they are both unity. The eigenvalues for $V^+V^- < 1$ lie on the unit circle, so the origin is nonhyperbolic, but this does not imply structural instability because orbits evolve under the map only for a finite time, after which they reach the sliding region.

8. Concluding remarks.

A vector formulation has been employed here wherever the analysis applies in general coordinate systems, for example, when $S^{\pm}$ are nonorthogonal. The

vector expressions also generalize naturally to higher dimensions. Specifically, the vector directions ∇h and $\mathbf{S}^{\pm}$ are well defined in n dimensions, respectively, by the codimension one switching surface Σ and the codimension two tangency sets $S^{\pm}$. Only the components $\nabla h \cdot \mathbf{X}$ and $\mathbf{s}^{\pm} \cdot \mathbf{X}$ play an essential role in a neighborhood where the maps (3.7) are valid. The unfolding parameter V^+V^- and the codimension two manifolds S and U will form a foundation for study in $n > 3$, where dynamics is possible within the tangency sets $S^{\pm}$, and parallel to the $n-3$ dimensional singular set $S^+ \cap S^-$.

Theorem 1(i) characterizes the attractivity of the two-fold singularity when the two vector fields $\dot{\mathbf{X}}^{\pm}$ form an obtuse angle at the singularity, in the plane spanned by orthogonal $\mathbf{s}^+$ and $\mathbf{s}^-$, measured on the side of the sliding region (the condition $V^+V^- > 1$). The state space contains regions of attraction and repulsion whose boundaries are a pair of invariant parabolic surfaces. A stable surface S encloses the escaping region, and orbits are repelled from the singularity as they approach it. An unstable surface U encloses the sliding region and orbits are attracted to the singularity as they depart it, until they impact the sliding region or approach S. Both surfaces are smooth except at their intersections with the crossing regions. Orbits of the sliding vector field take the form of a stable node at the singularity, though the node is reached in finite time, and the vector field is undefined at the singularity itself.

As the obtuse angle increases and the vector fields pass the point $V^+V^- = 1$ where they are colinear at the singularity, a bifurcation occurs which destroys the two invariant surfaces, and all orbits and sliding orbits flow away from the singularity. In this case (see Theorem 1(ii)), the two vector fields form an obtuse angle measured on the side of the escaping region (the condition $V^+V^- < 1$). All orbits originating close to the escaping region will eventually impact the sliding region, where the sliding vector field takes the form of a saddlepoint with its unstable manifold in the sliding region.

If one or both of the vector fields points into the sliding region at the singularity, $V^{\pm} \geq 0$, then all orbits reach the sliding region by crossing Σ at most once, after which they are repelled from the singularity. The case $V^+ = 0$ means that the vector field $\dot{\mathbf{X}}^+$ is perpendicular to its tangency set S^+ (similarly for the "$-$" case).

At the bifurcation point $V^+V^- = 1$ the vector fields are anticolinear at the singularity. The Teixeira singularity system then becomes an unfolding of the "fused-focus" in planar nonsmooth systems [9].

When $V^+ \to \infty$, the vector field $\dot{\mathbf{X}}^+$ is parallel to its own tangency set S^+ and forms a line of cusps; that case is too degenerate to be of interest here (similarly for V^-). If the tangency sets $S^{\pm}$ become tangent to each other at a codimension two point, we can appeal to our analysis for some basic intuition. The codimension two point splits under perturbation into a pair of two-fold singularities identified by Teixeira [16], one of the saddle type $V^+V^- > 1$ and one of the focal type $V^+V^- < 1$, and the dynamics around this singularity certainly merits further investigation.

The bifurcation in the sliding vector field observed in the bottom row of Figure 8 is related to Teixeira's "Q5-singularity case 2" [16]. We have shown how it occurs necessarily in the unfolding of the bifurcation.

Is the Teixeira singularity stable? On the question of asymptotic stability, we reiterate that the singularity is not a stationary point of the vector field. Asymptotic stability can only refer to the normalized sliding vector field (6.3), whose dynamics are different from the true

system. Instead we find that state space is separated into regions of attraction and repulsion, as given by the two regimes of Theorem 1 and the sliding dynamics of section 6. The invariant surfaces are locally asymptotically stable (S) and unstable (U), except at the singularity. The dynamics at the singularity is not uniquely defined in the Filippov convention, which we have followed here.

It is our position that *structural* stability in nonsmooth dynamical systems is not yet on as sound a footing as in smooth systems, and the Teixeira singularity is vital to this continuing investigation. To this end we have described the local dynamics and shown that it varies *smoothly* with the parameter V^+V^-, except at the bifurcation. This implies that the unfolding of the singularity in the parameter V^+V^- is structurally stable in the usual sense—intuitively that nearby orbits have the same topology in terms of the number of crossings, the tendency toward S and away from U, the impact in Σ, and so on.

We have shown that the characteristic dynamics of the Teixeira singularity involves bifurcations simultaneously in the crossing regions (equivalently, out of the switching surface) and in the sliding/escaping regions. A single parameter V^+V^- quantifies the relative direction of the vector fields at the singularity (or the jump in direction of the overall nonsmooth vector field through the singularity), controlling the bifurcation and determining domains of attraction. We have shown how the system behaves under perturbation at the bifurcation, and the effect of higher order terms here is currently in progress. Also of interest for applications is a closer look at the dynamics of the T_m map, including the number of iterations in each orbit and the dynamics around near misses of the sliding boundary, and comparison of this with physical models.

Appendix A. An explicit expression for the vector fields. At the singularity the x component of both vector fields vanishes, and locally we can expand to first order in the coordinates, giving

$$\left[\dot{x}^{\pm},\ \dot{\mathbf{x}}^{\pm}\right] \approx \left[\mathbf{x}\cdot\mathbf{a}^{\pm} + xb_x^{\pm},\ \mathbf{x}\mathsf{A}^{\pm} + x\mathbf{b}^{\pm} + \mathbf{c}^{\pm}\right] \tag{A.1}$$

in terms of constant scalars $b_x^{\pm}$, vectors $\mathbf{a}^{\pm}, \mathbf{b}^{\pm}$, and 2×2 matrices $\mathsf{A}^{\pm}$. We are interested only in quadratic tangencies, so we must impose the condition $c_y^+, c_z^- \neq 0$, and in general we will assume that $\mathbf{c}^{\pm}$ are nonparallel. Transversality of the tangent sets $S^{\pm}$ requires that $\mathbf{a}^{\pm}$ are also nonparallel. The unit vectors $\mathbf{s}^{\pm}$ satisfy

$$\mathbf{s}^{\pm}\cdot\mathbf{a}^{\pm} = 0, \tag{A.2}$$

and the choice of coordinates giving (2.7) is

$$y = -\mathbf{x}\cdot\mathbf{a}^{+} - xb_x^{+}, \qquad z = \mathbf{x}\cdot\mathbf{a}^{-} + xb_x^{-}. \tag{A.3}$$

This is a differentiable coordinate transformation given the condition

$$\begin{vmatrix} \mathbf{s}^{+}\cdot\mathbf{a}^{+} & \mathbf{s}^{+}\cdot\mathbf{a}^{-} \\ \mathbf{s}^{-}\cdot\mathbf{a}^{+} & \mathbf{s}^{-}\cdot\mathbf{a}^{-} \end{vmatrix} \neq 0. \tag{A.4}$$

The analysis thereafter applies on a neighborhood of the singularity satisfying

$$\mathbf{s}^{+}\cdot\left(\mathbf{x}\mathsf{A}^{\pm} + x\mathbf{b}^{\pm}\right) \ll c_y^{\pm} \quad \text{and} \quad \mathbf{s}^{-}\cdot\left(\mathbf{x}\mathsf{A}^{\pm} + x\mathbf{b}^{\pm}\right) \ll c_z^{\pm}. \tag{A.5}$$

Writing

$$\begin{aligned}\left[\dot{x}^+,\ \dot{\mathbf{x}}^+\right] &\approx \left[-y, \mathbf{c}^+\right],\\ \left[\dot{x}^-,\ \dot{\mathbf{x}}^-\right] &\approx \left[\ \ z, \mathbf{c}^-\right],\end{aligned} \tag{A.6}$$

we can rescale time independently in the $x > 0$ and $x < 0$ systems without altering the piecewise-smooth system topologically, letting $t \mapsto t/c_y^+$ for $x > 0$ and $t \mapsto t/c_z^-$ for $x < 0$, resulting in (2.10) by setting $a = 1/c_y^+$ and $b = 1/c_z^-$.

REFERENCES

[1] M. E. Broucke, C. Pugh, and S. Simic, *Structural stability of piecewise smooth systems*, Comput. Appl. Math., 20 (2001), pp. 51–90.

[2] R. Casey, H. de Jong, and J. L. Gouze, *Piecewise-linear models of genetic regulatory networks: Equilibria and their stability*, J. Math. Biol., 52 (2006), pp. 27–56.

[3] M. di Bernardo, C. J. Budd, A. R. Champneys, and P. Kowalczyk, *Piecewise-Smooth Dynamical Systems: Theory and Applications*, Springer-Verlag, New York, 2008.

[4] M. di Bernardo, F. Garofalo, L. Glielmo, and F. Vasca, *Switchings, bifurcations, and chaos in dc/dc converters*, IEEE Trans. Circuits Systems I Fund. Theory Appl., 45 (1998), pp. 133–141.

[5] A. F. Filippov, *Differential Equations with Discontinuous Righthand Sides*, Kluwer Academic Publishers, Dordrecht, The Netherlands, 1988.

[6] J. Y. Hung, W. B. Gao, and J. C. Hung, *Variable structure control—a survey*, IEEE Trans. Industrial Electronics, 40 (1993), pp. 2–22.

[7] M. Kunze, *Non-Smooth Dynamical Systems*, Springer-Verlag, Berlin, 2000.

[8] Y. A. Kuznetsov, *Elements of Applied Bifurcation Theory*, 2nd ed., Springer-Verlag, New York, 1998.

[9] Yu. A. Kuznetsov, S. Rinaldi, and A. Gragnani, *One-parameter bifurcations in planar Filippov systems*, Internat. J. Bifur. Chaos Appl. Sci. Engrg., 13 (2003), pp. 2157–2188.

[10] R. I. Leine and H. Nijmeijer, *Dynamics and Bifurcations of Non-Smooth Mechanical Systems*, Springer-Verlag, New York, 2004.

[11] H. E. Nusse, E. Ott, and J. A. Yorke, *Border-collision bifurcations: An explanation for observed bifurcation phenomena*, Phys. Rev. E (3), 49 (1994), pp. 1073–1076.

[12] N. S. Simic, K. H. Johansson, J. Lygeros, and S. Sastry, *Structural stability of hybrid systems*, in Proceedings of the European Control Conference, Porto, Portugal, 2001, pp. 3858–3863.

[13] F. Takens, *Forced oscillations and bifurcations*, in Applications of Global Analysis I, Comm. Math. Inst. Rijksuniv. Utrecht 3, Math. Inst. Rijksuniv. Utrecht, Utrecht, 1974, pp. 1–59.

[14] M. A. Teixeira, *On topological stability of divergent diagrams of folds*, Math. Z., 180 (1982), pp. 361–371.

[15] M. A. Teixeira, *Stability conditions for discontinuous vector fields*, J. Differential Equations, 88 (1990), pp. 15–29.

[16] M. A. Teixeira, *Generic bifurcation of sliding vector fields*, J. Math. Anal. Appl., 176 (1993), pp. 436–457.